2024 IEEE International Conference on Power, Electrical, Electronics and Industrial Applications (PEEIACON)
12-13 September, RUET, Rajshahi, Bangladesh

2024 IEEE International Conference on Power, Electrical, Electronics and Industrial Applications (PEEIACON) | 979-8-3315-1798-4/24/$31.00 ©2024 IEEE | DOI: 10.1109/PEEIACON63629.2024.10800121

Analysis of the Structural, Electronic, Mechanical and Optical Properties Through Density Function Theory of Bilayer Germanium Carbide

Md. Shizer Rahman
Department of Electrical and Electronic Engineering
Rajshahi University of Engineering & Technology, and
Bangamata Sheikh Fojilatunnesa Mujib Science & Technology University
Jamalpur-2012, Bangladesh
E-mail: shizer@bsfmstu.ac.bd

Md. Rasidul Islam
Department of Electrical and Electronic Engineering
Bangamata Sheikh Fojilatunnesa Mujib Science & Technology University
Jamalpur-2012, Bangladesh
E-mail: rasidul@bsfmstu.ac.bd

Ajay Krishno Sarkar
Department of Electrical and Electronic Engineering,
Rajshahi University of Engineering & Technology,
Rajshahi-6204, Bangladesh.
E-mail: aksarkar@eee.ruet.ac.bd

***Abstract*— Bilayer two-dimensional (2D) crystal have received substantial interest because of their remarkable features, including enhanced optical absorption, superconductivity, and adjustable bandgap. These properties surpass those of the currently available monolayer 2D materials. We primarily deal with two-dimensional bilayer germanium carbide's (2D-GeC) optical, vibrational, and electronic structure using an exact first-principles density functional theory (DFT) investigation. The electrical bandgap of bilayer 2D-GeC increases from 1.21 eV at the material's direct K-point to about 1.23 eV when the spin-orbit coupling (SOC) effect is included. The exceptional ability of bilayer 2D-GeC to absorb light in both the visible and infrared (IR) bands causes changes in its optical properties, including its real and imaginary dielectric spectra as well as its electron energy loss function (EELF).**

Keywords*— DFT, Bilayer 2D-GeC, Electronic properties, SOC, and Phonon properties

I. INTRODUCTION

Photovoltaics and nanoelectronics are two fields that have made extensive use in e academic and industrial field of two-dimensional (2D) materials because of their exceptional physical properties. In the first experimental discovery of a two-dimensional substance, graphene, the K-point is where bonding and anti-bonding orbitals converge [1]. Graphene possesses exceptional structural and electrical characteristics, making it very suitable for many applications , including gas sensors, corrosion inhibitors, and energy storage devices [2]. Because of its intrinsic lack of bandgap, monolayer graphene is significantly limited in the development of advanced electrical and logic circuits. However, a potentially successful approach is to produce bilayer graphene, which may provide an adjustable electronic bandgap and exhibit unique characteristics and phenomena. Bilayer 2D materials have significant applications in several domains including optoelectronics, nano-optics, piezoelectricity, catalysis, and anti-oxidation [3]. Thus, bilayer heterostructures offer several prospects in 2D materials, leading to a rapidly growing area of research. The bilayer 2D-GeC has a straight band gap, making it suitable for various optoelectronic digital circuits, including solar cells, photodiodes, light-emitting diodes (LEDs), and other applications. The spin-orbit coupling (SOC) is a significant determinant of the electrical characteristics of bilayer 2D materials. The correlation between the orbital velocity and spin orientation of electrons leads to a relativistic phenomenon known as the SOC effect. It is possible to adjust the electronic bandgap of materials, resulting in either an increase or a decrease, by including the SOC effect in calculations. Accounting for the SOC effect, graphene, which typically lacks a bandgap, may develop a bandgap of around 1 μeV [4]. The bandgap in lead (Pb)-based 2D perovskites might go down by about 1 eV because of the significant SOC effect, which can split the band structure [5]. The research on the electronic properties (bandgap and projected density of states(PDOS)) of bilayer 2D-GeC in the context of surface organic matter effects is currently lacking in knowledge. This is the case as of the present moment. To increase the practicability of bilayer 2D-GeC material in spintronic device technologies, it is very important to conduct additional research on the influence of spin-orbit coupling (SOC).

II. COMPUTATIONAL DETAILS

Quantum ESPRESSO, which is a package of software, is utilized in this investigation to do DFT-based first-principles computations. Using ultrasoft pseudopotentials and the Perdew-Wang exchange-correlation function, both of which operate under the local density approximation (LDA) [6], we can determine the structural relaxation of the system as well as the overall energy of the system. Double-layer 2D-GeC is used for computations. The monolayer of bilayer 2D-GeC is composed of a fundamental unit cell containing two atoms with the typical electron configurations of C [$2s^2$ $2p^2$] and Ge [$4s^2$ $4p^2$]. Our calculations assume that the cut-off values for kinetic energy are 40 Ry, which is approximately 410 eV, and the cut-off values for charge density are 200 Ry, which is approximately 2720 eV. The total energy convergence threshold and the force convergence threshold for ionic minimization are both set to 10^{-6} a.u. and 10^{-3} a.u. respectively, in the relaxation computations. Together, these values are used to determine ionic minimization. To determine band structure and state density, we make use of a

Monkhorst pack grid consisting of k-points that are centered on gamma. A sample of the irreducible Brillouin zone having dimensions of 6 × 6 × 1 is used to construct the grid. In order to remove any interactions between the image bilayers, the vacuum level is adjusted to 20 Å. The density functional perturbation theory (DFPT) is used to guarantee the dynamical steadiness of the bilayer 2D-GeC's lowest energy structure, which is necessary for phonon dispersion quality assessment [6]. The 2 × 2 × 2 dynamic matrix and the normal preserving pseudopotential with LDA were utilized to express phonons. According to Born and Huang, the method used at the Γ point took into consideration both longitudinal splitting and optical transverse modes. The Quantum Espresso program utilizes a DFPT computation to determine the second-order output to an electric field, generating the Raman peaks.

III. Result and Discussion

A. Structural properties

As a bilayer is formed by vertical stacking one layer on top of another may be constructed with just weak van der Waals forces holding them together. The electrons in the system will experience an extra potential. The interlayer electronic coupling is also greatly improved by quantum confinement and electronic states that are exposed to the surface. The additional potential and enhanced electronic coupling not only alter the inherent behavior of the layers but also give rise to many novel physical characteristics at the interface [7].

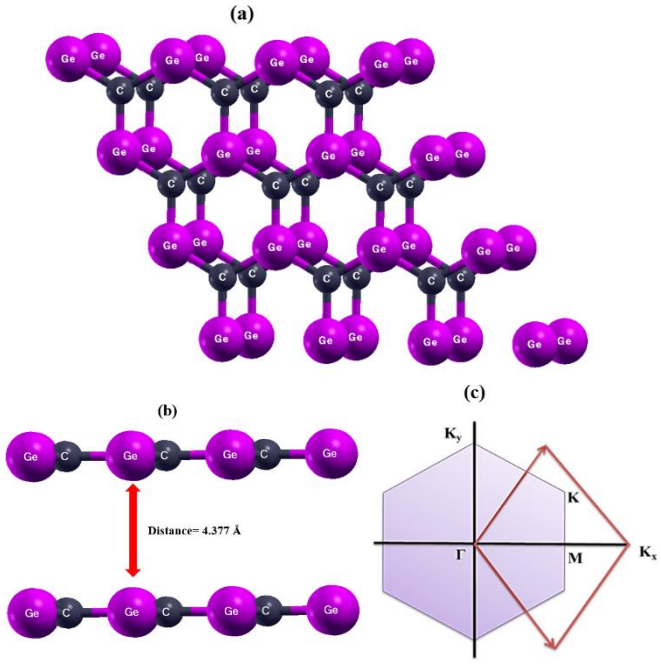

Fig. 1. Bilayer 2D-GeC's atomic structure (a) top view, (b) side view, and (c) high symmetry point.

To create the bilayer 2D-GeC unit cell in the original structure, carbon and germanium atoms were positioned in one layer on top of another. The geometry of the relaxed bilayer 2D-GeC exhibits a-a stacking patterns. The atoms of Ge and C in the upper and lowermost layers of 2D-GeC are aligned vertically. The first step in tuning the bilayer 2D-GeC 's structure is to account for surface effects, which alter an atom's structural characteristics. According to the data in Fig. 1(a), the relaxed structure depicts that the bilayer 2D-GeC stays coplanar. As long as the length of the Ge-C bond remains at 1.873 Å, the dynamically preferred planar structure will remain stable. There are 120 degrees between the bonds in Ge-C-Ge and C-Ge-C. We used the lattice parameter as the independent variable to compute total energy. The bilayer 2D-GeC structure's most stable lattice constant is 3.24 Å.

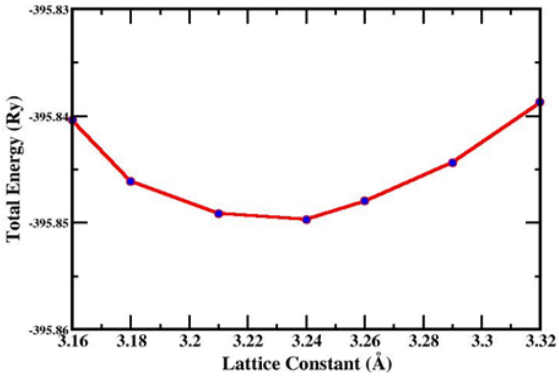

Fig. 2. Variation of bilayer 2D-GeC's per unit cell total energy concerning lattice constant

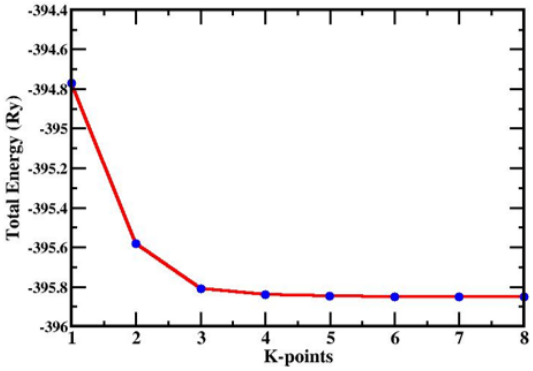

Fig. 3. Variation of bilayer 2D-GeC's per unit cell total energy concerning k-points.

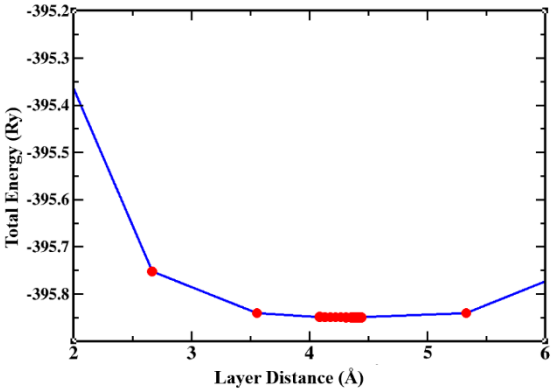

Fig. 4. Variation of bilayer 2D-GeC per unit cell total energy concerning bilayer distance.

The total energy will change about the lattice constant, as depicted in Fig. 2. Factors influencing the ideal configuration include the kinetic cut-off energy, the lattice constant, and the quantity of k-point objects in the Brillouin zone (BZ) loop. By adjusting the k-points and cut-off energy of the plane wave, the total energy has also been investigated under the PBE pseudopotential of the generalized gradient approximation. According to Fig. 3, k-point mesh 4 × 4 × 1 is enough for bilayer 2D-GeC's structure, which means that adequate k-

point sampling is necessary to ensure relative stability. Our research has focused on determining the optimum distance between layers in a bilayer 2D-GeC structure by evaluating the total energy using the layer distance only. When we increase the distance between the bilayer layers, the total energy decreases and eventually reaches its minimal value. After the bilayer layer distance reaches 4.377 Å, the total energy increases as the layer distance increases. The overall energy will vary in relation to the distance between layers, as seen in Fig. 4.

B. Electronic properties

As soon as we have reached a configuration of the system that is stable, we will concentrate on analyzing the electrical properties of this advantageous setup. In the beginning, the PBE functions were applied to determine the electrical band structure consistently. The electronic band structure of bilayer 2D-GeC is depicted in Fig. 5. This structure was determined through the utilization of PBE. As shown in Fig. 5(a), the K-point was found to be close to both the lowest and highest energy levels of the conduction and valence bands. Our analysis is predicated on the assumption of a direct band gap, which has a value of Eg = 1.21 eV with PBE. As a result, the energy band estimate that we have made involves this assumption. The electronic band structure of the bilayer 2D-GeC atom is composed of two bands that are composed of hybridized π and π* orbitals from Ge and C atoms. These bands split the Fermi level, which is initially set to zero.

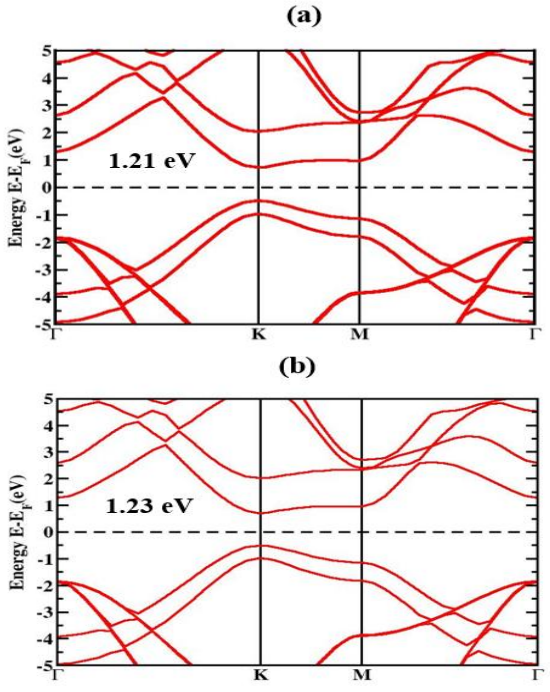

Fig. 5. Bilayer 2D-GeC's electronic band structure (a) without SOC effect and (b) with SOC effect where the Fermi level is marked by the dotted line.

By computing the PDOS, it is now feasible to have a better understanding of the electronic structure's component placement. A bilayer 2D-GeC is produced by connecting σ-bonds and π-bonds through the squared hybridization of orbitals in contrast to the ρ-bond, which is created by electrons from Ge-4p_z and C-2p_z, the ρ-bond is formed by electrons from germanium (Ge-4s, 4p_x, 4p_y) and carbon (C-2s, 2p_x, 2p_y). On the K-point, the π-band represents the conduction band and the π* band represents the valence band. These bands may be created by connecting the bonding and anti-bonding interactions of the Ge-4p_z and C-2p_z orbitals, respectively. Fig. 6(a), displays the electron contributions from two separate elements. The PDOS peaks in the valence band (VB) (-6 to -0.123 eV) and the conduction band (CB) (0.523 to 6 eV) are primarily composed of carbon, respectively. The Ge is mostly to blame for the PDOS conduction band (-0.1 to 5.6 eV) and valence band (-6 to -0.6 eV) peaks. The C-2p orbitals contribute somewhat, whereas the Ge-4p orbital is mostly accountable for the lowest conduction band. Conversely, the Ge-4p and Ge-4s orbitals contribute less, whereas the C-2p orbital predominantly governs the highest valence band.

The *l-s* coupling phenomenon arises from the combination of total spin angular momentum (*s*) and total orbital angular momentum (*l*). The symbol "*j*" is commonly used to represent the total angular momentum resulting from the *l-s* coupling. Multiple forms of (*l*+*s*), (*l*+*s*-*1*),... (*l*-*s*) are possible for "*j*". The probable values of the variable *j* range from $| l - s |$ to $| l + s |$. While *l*=0 and *j*=1/2 define the s orbitals, p orbitals may take on *j* values of 1/2 or 3/2 and have *l*=1. It is important to note that for all orbitals, s can take the values of +1/2 or -1/2.

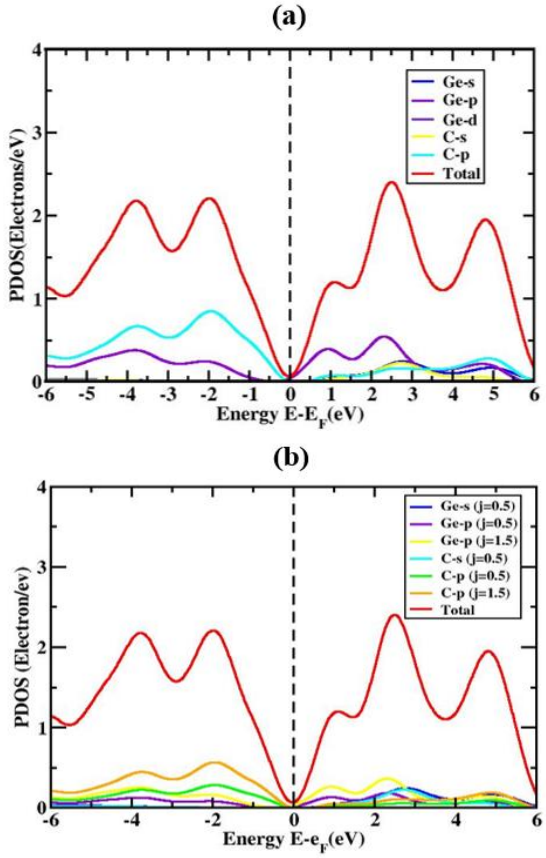

Fig. 6. The PDOS of bilayer 2D-GeC (a) without SOC effect, and (b) with SOC effect, demonstrating the unique impacts of each atomic orbital.

Fig. 5(b) displays the energy band structure and electrical density of states (DOS) when considering the SOC effect. The projected K-point of the BZ's energy gap using the PBE function is around 1.23 eV. When the SOC is considered with PBE, we find that the bandgap increases by 20 meV. The bandgap value we have determined closely aligns with the values published in earlier publications that used PBE

functionals [8]. In bilayer 2D-GeC semiconductors, for example, the p orbital top of the valence bands results in $l = 1$ when there is no SOC taken into consideration. Equations j = 3/2 and j = 1/2 indicate the total angular momentum, which is created when the electrical states take into account the SOC effect. Considering this, an energy gap, which is referred to as the SOC gap, emerges between the $j = 3/2$ and $j = 1/2$ states that have recently been introduced. Fig. 6(b), which shows that two more branches are obtained because of these higher angular momentums. Due to the presence of C atoms, the CB voltage range of 0.55 to 6 eV and the VB voltage range of -6 to -0.12 eV both exhibit maxima for j=1/2 and j=3/2. Furthermore, both the CB voltage range of 0.1 to 6 eV and the VB voltage range of -5 to -0.8 eV exhibit maxima for each angular momentum $j = 1/2$ and $j = 3/2$, which can be attributed to the contribution of Ge atoms. Nearly no contribution comes from the d-orbital of Ge atoms.

C. *Vibrational properties*

A material's thermodynamic stability can be assessed through the analysis of phonon dispersion behavior. In contrast to negative or unreal frequencies, which indicate crystal structure instability, positive phonon frequency modes indicate a structurally stable dynamic state [5]. According to the theory of lattice dynamics, this makes sense. To demonstrate dynamic stability, we focused on the Γ- K - M -Γ points and used the DFPT technique to analyze the phonon band diagram of bilayer 2D-GeC. In Fig. 7, six separate bilayer 2D-GeC phonon modes are displayed, illustrating the corresponding phonon band structure. Acoustic phonons are the three lowest phonon modes: LA, TA, and ZA. The three remaining optical phonon modes are LO, TO, and ZO. Acoustic phonons are denoted by A, optical phonons by O, longitudinal modes by L, transverse modes by T, and flexural or out-of-plane vibration modes by Z. Since there are no negative frequencies across the BZ in the phonon band structure of bilayer 2D-GeC (Fig. 7), it is suggested that bilayer 2D-GeC possesses a dynamically stable structure.

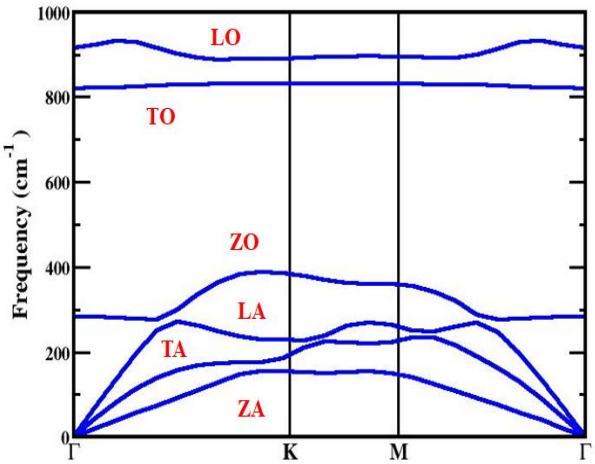

Fig. 7. Bilayer 2D-GeC's phonon band structure.

D. *Optical properties*

This section uses the PBE functional and DFPT to determine the optical features. specifically the dielectric function (DF) and EELF. The complex Dielectric constant $\varepsilon(\omega) = \varepsilon_1(\omega) + i\varepsilon_2(\omega)$ shows how the frequency (ω) dependent dielectric constant imaginary script down into real $\varepsilon_1(\omega)$ and imaginary $\varepsilon_2(\omega)$ when light hits the materials. By applying the Kramers-Kronig dispersion relationships, we have calculated the DF's real and imaginary components. A formula was used to derive the imaginary dielectric function $\varepsilon_2(\omega)$ [9]:

$$\varepsilon_2(\omega)=\frac{Ve^2}{2\pi\hbar m^2\omega^2} \times \int d^3k \sum\left|<\varphi_c|p|\varphi_v>\right|^2 \delta(E_c-E_v-\hbar\omega) \quad (1)$$

where the unit cell volume is denoted by V. The decreased Planck's constant is "$\hbar$", p is the momentum operator φ_c stand wave functions for conduction and φ_v stand for wave functions for valence bands.

a function's real portion $\varepsilon_1(\omega)$can be represented as [9]:

$$\varepsilon_1(\omega)=1+\frac{2}{\pi}P\int_0^{\infty}\frac{\varepsilon_2(\omega')\omega'}{\omega'^2-\omega^2}d\omega \quad (2)$$

P is the prime integral value in this case.

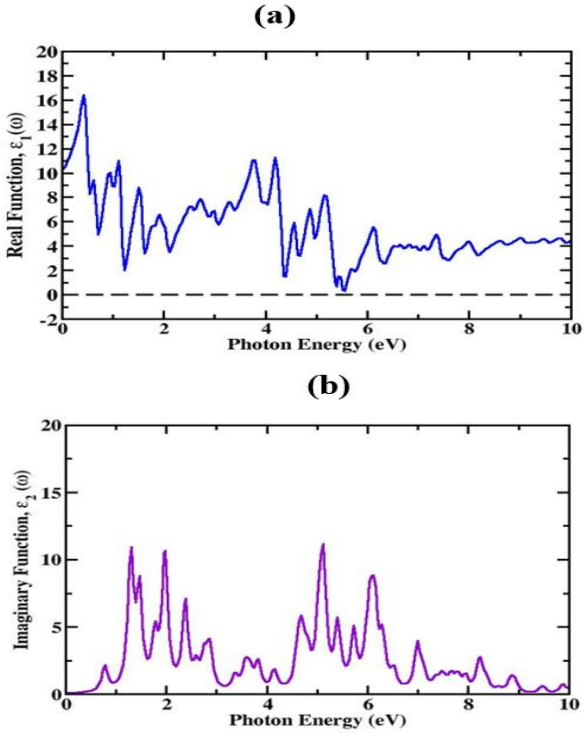

Fig. 8. Bilayer 2D-GeC's (a) The real and (b) imaginary function.

The optical properties of incoming light that is polarized perpendicular to the bilayer plane were the main focus of the investigation. The real portion of the dielectric function $\varepsilon_1(\omega)$ shows the electronic polarizability and dispersion effects of the material being studied. The segment's most relevant property is the magnitude of $\varepsilon_1(\omega)$) at ω=0. The parallel orientation of the bilayer 2D-GeC is marked by considerable electronic polarizability, as seen by its estimated $\varepsilon_1(0)$ value of approximately 10.38. The steep decrease in $\varepsilon_1(\omega)$ as photon energy continues to rise indicates that there is less chance of substantial light absorption in this energy range and, thus, less chance of great light-absorbing capacity in this range. The remarkable refractive index and semiconducting properties of the bilayer 2D-GeC are demonstrated by its several positive peaks in $\varepsilon_1(\omega)$ value. As a result, we found that bilayer 2D-GeC works wonderfully for infrared optical applications. Fig. 8(a) and 8(b) demonstrate that the real and imaginary dielectric constants are present. The imaginary dielectric function $\varepsilon_2(\omega)$ can be used to find out information

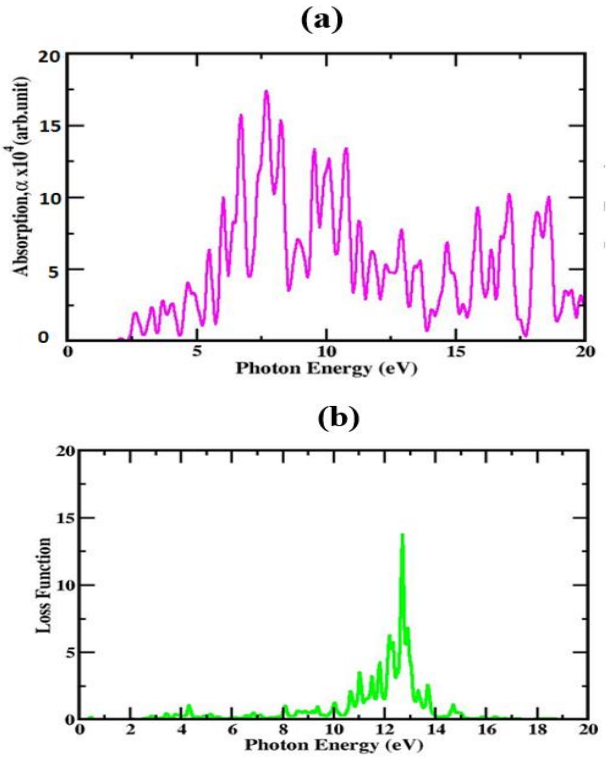

Fig. 9. Bilayer 2D-GeC's (a) Absorption coefficient and (b) loss function.

about the electronic bandgap and absorption loss of materials due to inter-band transmission around the Fermi level. The peaks seen in the imaginary part of the dielectric function are explained by carrier transitions between VB and CB. The band structure of a system is intimately associated with its imaginary $\varepsilon_2(\omega)$. The main peaks of $\varepsilon_2(\omega)$ for bilayer 2D-GeC at 5.12 eV photon energy at the highest optical points of 11.71 eV. The expected bandgap values are consistent with the planned fundamental absorption peak of 7.71 eV for bilayer 2D-GeC. On top of that, the visible region shows a more pronounced initial optical absorption peak. Without a doubt, this peak proves that the bilayer 2D-GeC is very suitable for use in optoelectronic devices. Both the 2nd and 3rd major peaks for bilayer 2D-GeC are captured by the visible zone as well. Bilayer 2D-GeC is believed to be an attractive material for visible light absorption since the largest imaginary DF peaks remain in the visible region within the incoming photon energy range of 1.75 eV to 3.3 eV. Considering the real and imaginary components of the absorption coefficient, the dielectric functions like this:

$$\alpha(\omega) = \sqrt{2}\left(\sqrt{\varepsilon_1^2(\omega) + \varepsilon_2^2(\omega)} - \varepsilon_1(\omega)\right)^{1/2} \quad (3)$$

the absorption coefficient and the photon frequency are represented by α and ω, respectively Fig. 9(a) shows the optical absorption coefficient, which is one measure of a material's light transmission through it. An optoelectronic device can only use materials that reveal how to maximize the efficiency with which solar energy is converted. As seen in Fig. 9(a), the absorption coefficient for bilayer 2D-GeC varies with photon energy. In solar cell applications, the early absorption peak is significant since it primarily reveals the material's light-emitting area [10]. The bilayer 2D-GeC exhibited absorption in the visible light domain, which was determined by the location of the first peak.

Additionally, the EELF for the bilayer 2D-GeC was calculated using the incoming photon spectra. Frequency-dependent L (ω) is the energy emitted by electrons moving across a dielectric material. This can be determined by applying the complex dielectric relation:

$$L(\omega) = Im\left(\frac{-1}{\varepsilon(\omega)}\right) = \frac{\varepsilon_2(\omega)}{\varepsilon_1^2(\omega) + \varepsilon_2^2(\omega)} \quad (4)$$

Fig. 9(b), displays the EELF for a bilayer 2D-GeC. The graphs show that the electron energy loss and resonance in bilayer 2D-GeC mostly happen in the UV region. Photon loss in bilayer 2D-GeC is less variable and limited to a given energy scale, making it a promising material for photosensitive storage devices.

E . Thermal Properties

To study thermal properties at high pressure and temperature, a quasi-harmonic Debye approximation is necessary. The structural parameters at T=0 and P=0 may be found using this static approximation by first determining the total energy in proportion to the primitive cell volume (E-V). The macroscopic properties are thereafter defined in terms of T in accordance with the widely accepted thermodynamic correlations. It is also possible to estimate thermal properties with high precision using the quasi-harmonic approach from 0 to 800 K. As seen in Fig. 10 (a), the thermal effect is represented by the heat capacity C_v. At a steady volume, the C_v approaches the limits set by Dulong and Petit 75.9 $J.mol^{-1}K^{-1}$ at 800 K. In low-temperature conditions, the C_v increases as a function of T^3. However, long-term experimental testing was needed to identify the heat potential, which is determined by intermediate temperature atomic dynamics [11].The temperature variation of the bilayer 2D-GeC material from 0 K to 800 K is also shown in Fig. 10 (b). At 800K, the best thermal entropy is observed, and the value is 216 $J.mol^{-1}K^{-1}$. The fact that entropy is still changing, and we discover that it increases with temperature. From Fig. 10 (b) also represent that when temperature increases then the entropy is also increase and the maximum entropy present at 800 K.

F. Mechanical properties

Because they provide important details about the crystal's exposure, the bilayer 2D-GeC elastic constants were computed. We determined the C_{11}, C_{12} and C_{44} elastic constants. We found that C_{11}=355.3, C_{12}=109.6 and C_{44}=33.54. We also found that the shear modulus (B) is 61.8 (GPa), bulk modulus (G) is 27.8 (GPa), Young Modulus is (E) 63.7 (GPa), critical value B/G =2.22, Poisson's ratio (ϑ)=0. 271.We Calculate the value of C_{12}-C_{44} is 321.76. The following are the famous Born stability parameters that are believed to reflect the mechanical stability of bilayer 2D-GeC:

$C_{11} > 0$, $C_{44} > 0$, $C_{11} + 2C_{12} > 0$, $C_{11} - C_{12} > 0$

To estimate the ductile and brittle qualities of the material, one uses the C_{12}-C_{44} number, which is termed the Cauchy pressure. Positivity of the Cauchy pressure is an indicator of

the ductility of the material. To distinguish between ductile and brittle components, Pugh et al. [12] proposed the conventional formula, Pugh's ratio. There is a critical value of 1.75 for the shear modulus (B) relative to the bulk modulus (G). Materials having a ratio greater than 1.75 are ductile, whereas those below 1.75 are brittle. The computed values indicate that the bilayer 2D-GeC are ductile. The Poisson's ratio (ϑ) can also be used to define the difference between ductile and brittle materials. It is important to note that ϑ is larger for ductile materials compared to delicate ones, where it is 0.26 or less. With a ϑ value higher than 0.26, these 2D-GeC are ductile materials. Thus, it's clear that our technology will help make for device fabrication with a highly ductile material.

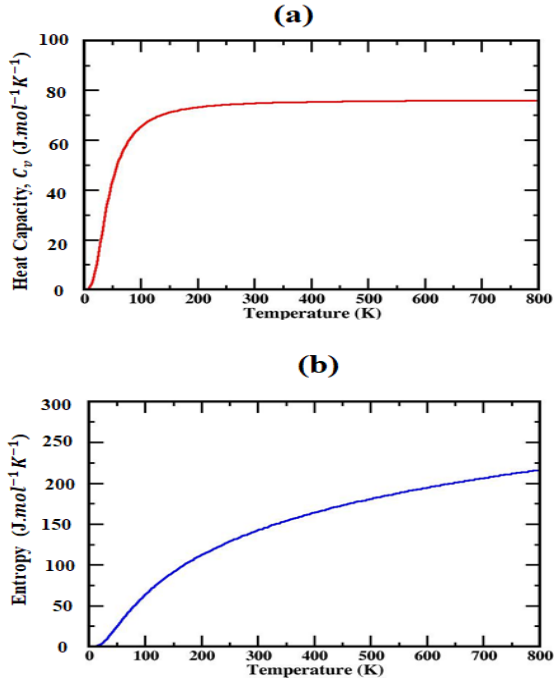

Fig. 10. (a) Heat Capacity Vs Temperature, (b) Entropy Vs Temperature curve of 2D-GeC.

IV. Conclusion

Using first-principles simulations, the optical, electrical, and vibrational characteristics of bilayer 2D-GeC are investigated thoroughly. The electronic energy band structure and state densities within the energy range of 1.21 eV exhibit a direct bandgap when using PBE, as anticipated by DFT. However, the existence of the SOC effect causes this bandgap to increase to 1.23 eV. The PDOS shows Ge and C atoms' distinct contributions to the structure. The CB is filled with Ge atoms, whereas the VB is filled with C atoms. Phonon dispersion behavior was examined to ascertain the materials' thermodynamic stability. The analysis of the dielectric constant's real, imaginary, and loss functions suggests that bilayer 2D-GeC has great promise for applications in optoelectronic and photosensitive storage devices. But the primary obstacle to the exploration of practical applications based on the 2D bilayers heterostructure family is the large-area single crystal and the enormous manufacture of clean interfaces.

References

[1] M. Shahrokhi and C. Leonard, "Tuning the band gap and optical spectra of silicon-doped graphene: Many-body effects and excitonic states," *J. Alloys Compd.*, vol. 693, pp. 1185–1196, 2017.

[2] A. Bhat, S. Anwer, K. S. Bhat, M. I. H. Mohideen, K. Liao, and A. Qurashi, "Prospects challenges and stability of 2D MXenes for clean energy conversion and storage applications," *npj 2D Mater. Appl.*, vol. 5, no. 1, p. 61, 2021.

[3] K. Yasuda, X. Wang, K. Watanabe, T. Taniguchi, and P. Jarillo-Herrero, "Stacking-engineered ferroelectricity in bilayer boron nitride," *Science (80-.).*, vol. 372, no. 6549, pp. 1458–1462, 2021.

[4] Y. Yao, F. Ye, X.-L. Qi, S.-C. Zhang, and Z. Fang, "Spin-orbit gap of graphene: First-principles calculations," *Phys. Rev. B*, vol. 75, no. 4, p. 41401, 2007.

[5] M. Pandey, K. W. Jacobsen, and K. S. Thygesen, "Band gap tuning and defect tolerance of atomically thin two-dimensional organic–inorganic halide perovskites," *J. Phys. Chem. Lett.*, vol. 7, no. 21, pp. 4346–4352, 2016.

[6] S. Baroni, S. De Gironcoli, A. Dal Corso, and P. Giannozzi, "Phonons and related crystal properties from density-functional perturbation theory," *Rev. Mod. Phys.*, vol. 73, no. 2, p. 515, 2001.

[7] Y. Cheng, C. Huang, H. Hong, Z. Zhao, and K. Liu, "Emerging properties of two-dimensional twisted bilayer materials," *Chinese Phys. B*, vol. 28, no. 10, p. 107304, 2019.

[8] M. R. Islam, A. S. M. J. Islam, K. Liu, Z. Wang, S. Qu, and Z. Wang, "Strain engineering on the electronic, phonon, and optical properties of monolayer boron antimonide," *Chem. Phys.*, vol. 551, no. March, p. 111334, 2021.

[9] M. A. Fadla, B. Bentria, T. Dahame, and A. Benghia, "First-principles investigation on the stability and material properties of all-inorganic cesium lead iodide perovskites CsPbI3 polymorphs," *Phys. B Condens. Matter*, vol. 585, no. February, p. 412118, 2020.

[10] M. N. Islam, M. A. Hadi, and J. Podder, "Influence of Ni doping in a lead-halide and a lead-free halide perovskites for optoelectronic applications," *AIP Adv.*, vol. 9, no. 12, pp. 1–9, 2019.

[11] M. R. Islam, B. K. Moghal, and R. Moshwan, "Tuning the electronic, optical, and thermal properties of cubic perovskites CsPbCl3-nBrn (n= 0, 1, 2, and 3) through altering the halide ratio," *Phys. Scr.*, vol. 97, no. 6, p. 65704, 2022.

[12] S. F. Pugh, "XCII. Relations between the elastic moduli and the plastic properties of polycrystalline pure metals," *London, Edinburgh, Dublin Philos. Mag. J. Sci.*, vol. 45, no. 367, pp. 823–843, 1954.